Food & Medicine Homology

ISSN 3006-6867 (print); 3006-4252 (online)
https://doi.org/10.26599/FMH.2026.9420103

Research Article

# Natural active ingredient identification from food and medicine homology products *Achyranthis bidentatae radix* and *Saururus chinensis* in hypertrophic cardiomyopathy and hypertension by bioinformatics and CADD approaches

Dan Xiao[1, 2, †], Tong Lu[3, †], Ming Jiang[4, †], Min-Hui Li[5], Denis Baranenko[6], Liudmila Natdochii[6], Wei-Hong Lu[1], Hui Li[4] (✉), Wei-Wei Jia[7] (✉)

[1] *National and Local Joint Engineering Laboratory for Synthesis Transformation and Separation of Extreme Environmental Nutrients, Harbin Institute of Technology, Harbin 150001, China*
[2] *Zhengzhou Research Institute, Harbin Institute of Technology, Zhengzhou 450007, China*
[3] *Medical Technology Department, Qiqihar Medical University, Qiqihar 161006, China*
[4] *Qiqihar Medical University, Qiqihar 161003, China*
[5] *Inner Mongolia Traditional Chinese & Mongolian Medical Research Institute, Hohhot 010010, China*
[6] *School of Life Sciences, Faculty of Ecotechnologies, ITMO University, St. Petersburg 197101, Russia*
[7] *Department of Basic Medicine School, Qiqihar Medical University, Qiqihar 161006, China*
† *Dan Xiao, Tong Lu, and Ming Jiang contributed equally to this work.*

**Received:** 19 July 2024 / **Revised:** 14 August 2024 / **Accepted:** 18 August 2024

**Abstract:** Hypertrophic cardiomyopathy (HCM) and hypertension often coexist, sharing common etiological factors and pathological mechanisms. Both traditional and modern medicine have explored food and medicine products for their treatment This study examines the therapeutic potential and mechanisms of *Achyranthis bidentatae radix* and *Saururus chinensis*, two natural products used in food and medicine homology, in addressing HCM and hypertension. Bioinformatics and computer-aided drug design (CADD) approaches were utilized to identify active ingredients and mechanisms. *In vivo* and *ex vivo* experiments were performed to validate the pharmacological effects under conditions mimicking HCM and hypertension. Disease-related genes were identified using GeneCards and DisGeNET, while key components were identified via Traditional Chinese Medicine Systems Pharmacology Database (TCMSP). A total of 62 disease-related genes were identified, with 20 significant components for *A. bidentatae radix* and 5 for *S. chinensis* Intersection analysis highlighted 18 common target genes involved insulin-like growth factor 1 receptor (*IGF1R*), insulin receptor (*INSR*), insulin (*INS*), Matrix Metallopeptidase 9 (*MMP9*), signal transducer and activator of transcription 3 (*STAT*), were confirmed through real-time PCR *in vivo*. Molecular docking studies demonstrated direct interactions between quercetin and IGF1R, INSR, MMP9, and between inophyllum E and INS. Molecular dynamics simulations showed favorable binding of quercetin with INSR. Quercetin exhibited promising drug-likeness and therapeutic potential in angiotensin II-treated cardiomyocytes. In conclusion, quercetin, identified as active component in *A. bidentatae radix* and *S. chinensis*, shows promising therapeutic effects against HCM and hypertension. These findings highlight the potential of these natural products in cardiovascular disease management through targeted molecular interactions. Future research should explore the nature products with long-term effects in comprehensive cardiovascular disease treatment.

**Keywords:** *Achyranthis bidentatae radix*; *Saururus chinensis*; hypertrophic cardiomyopathy; hypertension

**Citation:** Xiao D., Lu T., Jiang M., et al. Natural active ingredient identification from food and medicine homology products *Achyranthis bidentatae radix* and *Saururus chinensis* in hypertrophic cardiomyopathy and hypertension by bioinformatics and CADD approaches. *Food & Medicine Homology*, 2026, 3: 9420103. https://doi.org/10.26599/FMH.2026.9420103

## 1 Introduction

Hypertrophic cardiomyopathy (HCM) is frequently associated with severe complications, including atrial fibrillation, heart failure, and arrhythmias. Notably, approximately 62% of HCM patients also present with concomitant hypertension[1], which complicates clinical management and underscores the need for effective therapeutic strategies. In the early stages, both HCM and hypertension can be asymptomatic, with rapid myocardial hypertrophy often occurring following the onset of hypertension[2].

© National R&D Center for Edible Fungus Processing Technology 2025. Published by Tsinghua University Press. This is an open access article under the CC BY-NC-ND license (http://creativecommons.org/licenses/by-nc-nd/4.0/).

Address correspondence to Hui Li, lihui314220@126.com; Wei-Wei Jia, phyllis8459@163.com

The search for safe and effective treatments for patients with hypertensive HCM remains ongoing, highlighting the importance of complementary interventions.

The intefration of traditional Chinese medicine (TCM) into combined therapeutic regimens is based on their synergistic effects and potential to reduce adverse reactions[3]. *Saururus chinensis* and *Achyranthis bidentatae radix* are two TCM herbs recognized for their dual role as food and medicine. They are traditionally employed in management of various conditions, including rheumatoid arthritis[4], due to their abilities to promote blood circulation, resolving stasis[5], reducing swelling[6], and alleviating pain[7].

In TCM, *A. bidentatae radix* and *S. chinensis* are commonly used to treat various cardiovascular diseases. *A. bidentatae radix*, which is bitter and sour in taste, and neutral in nature, is associated with the liver and kidney meridians. It is known for its abilities to tonify the liver and kidneys, strengthen bones and muscles, promote blood circulation, regulate menstruation, and induce diuresis to alleviate stranguria. Modern research has validated the pharmacological effects of *A. bidentatae radix*, including antihypertensive, lipid-lowering, anti-inflammatory, and analgesic properties[8]. *S. chinensis*, characterized by its pungent and bitter taste and cold in nature, is linked with the lung, liver, and stomach meridians. Traditionally, it is used to clear heat and detoxify, promote diuresis, reduce swelling, and invigorate blood circulation to eliminate stasis. Conteporary studies have confirmed its significant anti-inflammatory, antibacterial, and antihypertensive effects[9].

From a TCM perspective, *A. bidentatae radix* and *S. chinensis* offer distinct advantages in treating HCM and hypertension. In TCM, HCM is often attributed to qi stagnation, blood stasis, and phlegm-dampness obstruction. *A. bidentatae radix*, by promoting blood circulation, removing stasis, and unblocking the channels, may effectively improve myocardial blood supply and reduce myocardial hypertrophy[10]. *S. chinensis*, through its heat-clearing and detoxifying, diuretic, and swelling-reducing properties, aids in lowering blood pressure and reducing cardiac burden[9].

Modern medical research further elucidates the mechanisms by which *A. bidentatae radix*, and *S. chinensis* exert their effects. *A. bidentatae radix* acts through multiple pathways, including anti-fibrosis, antioxidant activity, and inhibition of the renin-angiotensin-aldosterone system, to slow the progression of myocardial hypertrophy[10]. *S. chinensis,* with its anti-inflammatory, antibacterial, and antihypertensive properties, assists in controlling hypertension and protecting the cardiovascular system[11]. Additionally, both herbs are gaining attention for their applications in functional foods. *A. bidentatae radix* due to its rich nutritional components and pharmacological effects, is widely used in health foods aimed at enhancing physical fitness and cardiovascular health[12]. *S. chinensis*, known for its heat-clearing, detoxifying, and blood pressure-lowering effects, is utilized in the production of various functional beverages and health products, contributing to blood pressure regulation and overall health promotion[9]. The selection of this herbal pair is deeply rooted in TCM theory, where herbs are often combined to enhance therapeutic outcomes. Their combination is based on ancient TCM formulations designed to synergistically treat conditions, especially cardiovascular diseases. The pharmacological properties and traditional use of *S. chinensis* and *A. bidentatae radix* suggest a promising complementary approach to the treatment of cardiovascular diseases, particularly in patients with hypertensive HCM.

Bioinformatic network analysis leverages the "disease-gene-target-drug" interaction network to comprehensively assess the impact of drugs on disease networks[8]. Computer-aided drug design (CADD) techniques further provide a scientific foundation for the future development and clinical application of TCM by evaluating the binding modes, receptor affinities, and molecular potential of drugs with high speed and accuracy[13,14]. The integration of bioinformatics and CADD methods has proven effective across various therapeutic areas. For instance, bioinformatics tools have been employed to analyze the structure and sequence of the HIV protease enzyme, while CADD has facilitated the design of inhibitors that effectively bind to and inhibit this enzyme[15]. In oncology, bioinformatics is used to identify potential drug targets by analyzing genetic and proteomic data, followed by CADD-driven design of molecules that interact with these targets, thereby optimizing efficacy and minimizing side effects[16]. Similarly, in neurodegenerative diseases such as Alzheimer's, bioinformatics helps identify key proteins involved in disease progression, and CADD is utilized to design small molecules that modulate the activity of these proteins[17]. For cardiovascular drugs, bioinformatics tools analyze genetic variations associated with cardiovascular diseases, and CADD methods are then employed to design drugs targeting these specific genetic variations[18]. In our pilot study, we aimed to investigate the active ingredients of *S. chinensis* and *A. bidentatae radix* for their therapeutic potential against HCM and hypertension using bioinformatic and CADD approaches.

## 2 Materials and methods

### 2.1 Drugs

Angiotensin II (AngII) was purchased from Sigma-Aldrich Co. (Sigma Aldrich, St. Louis, MO, USA, CAS: 4474-91-3) and dissolved into 5% into aqueous solution of acetic acid. Quercetin (≥98% in purity, molecular weight: 302.24) was purchased from Sigma- Aldrich Co. (Sigma Aldrich, St. Louis, MO, USA, CAS: 117-39-5). For *in vitro* experiments, quercetin was dissolved in dimethyl sulfoxide (DMSO, Sigma, Louis, MO, USA). In parallel, control cells were treated with a non-toxic final concentration of 0.1% DMSO.

### 2.2 Bioinformatics

#### 2.2.1 *Genes associated with HCM and hypertension*

GeneCards (https://www.drugBank.ca/) and DisGeNET (https://www.disgenet.org/) databases were used to search for genes associated with "hypertrophic cardiomyopathy" and "hypertension" as keywords. The genes that influenced both HCM and hypertension were identified by taking the intersection by Venn diagram (https://bioinfogp.cnb.csic.es/tools/venny/index2.0.2).

#### 2.2.2 *Acquisition of active ingredients*

The TCM Systems Pharmacology Database and Analysis Platform (TCMSP) (http://tcmspw.com/tcmsp.php) and the Traditional Chinese Medicine Integrated Database (ETCM) (http://www.tcmip.cn/ETCM/index.php/Home/Index/index.html) were used to search for *A. bidentatae radix* and *S. chinensis*. Active ingredients of *A. bidentatae radix* and *S. chinensis* were identified based on their oral bioavailability (OB) ≥ 30% and drug-likeness (DL) ≥ 0.18. The BATMAN database (http://bionet.ncpsb.

org/batman-tcm/, score cutoff of 20, $P < 0.05$) and SwissTargetPrediction (http://www.swisstargetprediction.ch/, with probability greater than 0) was used to predict the targets corresponding to the chemical small molecules. The PubChem database (https://pubchem.ncbi.nlm.nih.gov/) was used to convert all compounds into standard canonical SMILES format.

#### 2.2.3 *Construction of protein-protein interaction network*

Venn diagram was used to obtain the intersection of both diseases and ingredients. The STRING 11.5 database was used to analyze the protein-protein interactions. The Cytoscape 3.8.2 software was used to construct the protein-protein interaction networks (PPI) network analysis of the intersecting targets.

#### 2.2.4 *Gene Ontology and Kyoto Encyclopedia of Genes and Genomes (KEGG) pathway enrichment analysis*

The intersecting targets were imported into Cytoscape. ClueGO and CluePedia plugins were used for Geneontology (GO) functional clustering analysis of the targets with parameters set as Number of genes = 4 and Min percentage = 4.0. The results were displayed as network graphs and bar charts.

The targets were subjected to KEGG pathway enrichment analysis using the cluster Profile R package (version 4.4.4). The functional pathways involving the key genes were explored, and the top 10 significantly enriched pathways were selected for bubble chart visualization.

#### 2.2.5 *Construction of herb-ingredient-target-pathway network*

Cytoscape was used to construct a pharmacological network to demonstrate the pathway regulation mechanisms of the important ingredients' related target proteins in the herbal formula.

### 2.3 CADD approaches

#### 2.3.1 *Molecular docking*

Molecular docking was performed between the key target proteins and their corresponding ingredients in PPI network based on the connectivity rankings. The PDB (http://www.rcsb.org/) format files of the protein-ligand complexes were downloaded. The obtained target protein was isolated by removing other ligands and water molecules using the Pymol software (Version 2.0, Schrödinger, LLC.). The molecular structures in SDF format were downloaded from the PubChem Compound database (https://pubchem.ncbi.nlm.nih.gov/) and converted to PDB format using pymol (Version 2.5). Autodock software was used to study the potential molecular docking between the ingredients and target proteins.

#### 2.3.2 *Molecular dynamics simulation*

The simulations were performed using Gromacs version 2022.3. The small molecules were pre-processed using AmberTools22 to add the general amino acid force field (GAFF), and Gaussian16W was used to add hydrogen atoms and calculate the restrained electrostatic potential (RESP) charges. The simulation conditions were set at a static temperature of 300 K and atmospheric pressure (1 bar). The Amber99sb-ildn force field was used, with water molecules (Tip3p water model) as the solvent. Appropriate amounts of $Na^+$ ions were added to neutralize the total charge of the simulation system. The duration of the simulation was 100 ps. Finally, a free molecular dynamics simulation was run for a total duration of 100 ns. After completing the simulation, the software's built-in tools were used to analyze the trajectories and calculate data such as the root mean square deviation (RMSD) of the amino acid movement trajectories and the binding free energy (MMGBSA).

#### 2.3.3 *DL evaluation*

DL evaluations were performed by appropriate modules in ADMETlab (version 2.0), including properties of ADME characteristics, number of violations of DL rules, and toxicity.

### 2.4 Animal model establishment

All mice (QMU-AECC-2019-69) were fed for 1 week acclimatization, and randomly divided into two parts. The experimental protocols involving animals were approved by the Animal Ethical Care Committee of Harbin Institute of technology (Harbin, China; approval No. IACUC-2024018) and complied with the Guide for the Use and Care of Laboratory Animals published by the USA National Institutes of Health (NIH Publication No 85-23, revised 1996). Group I: Control group. Animals were administered vehicle only (saline) and normal diet; Group II: Cardiac remodeling group, which divided into 1) isoproterenol (ISO) group, animals were treated with ISO only (5 mg/kg, subcutaneously) for 14 consecutive days; 2) transaortic constriction (TAC) group for 4 weeks; 3) *N*-nitro-*L*-argininem-ethylester (*L*-NAME) group with 0.5 g/L daily water for 4 weeks. Heart tissues were than collected for subsequent experiments.

### 2.5 Cell culture and treatment

Primary cardiomyocyte isolation was performed as previously indicated[19]. Cells were supplemented with DMEM (Sigma, Louis, MO, USA) supplied with 10% fetal bovine serum (Gibco, Carlsbad, CA, USA) and 1% penicillin/streptomycin (100 μg/mL) in 5% $CO_2$ at 37 °C. After a 2-h differential adhesion, non-adherent cells were collected and seeded in new culture dishes. After 48 h culture, the cardiomyocytes were then divided into three groups: Control, AngII, and AngII + quercetin group (AngII + Q).

### 2.6 Real-time PCR

The left ventricular tissue was thoroughly minced. Total RNA was harvested from cells using TRIzol reagent (Invitrogen, Carlsbad, CA, USA) as previously mentioned[19]. Primer pairs were designed by RiboBio Co., Ltd. (Guangzhou, Guangdong, China) and presented in Table S1. *Gapdh* was used as an internal control. Relative mRNA levels were calculated by $2^{-\Delta\Delta Ct}$. The groups were designed as: Control, AngII, and AngII + Q.

### 2.7 Statistical analysis

All values are presented as mean ± SEM. Statistical comparisons were performed by Student's *t*-test between two groups or one-way ANOVA for multiple comparisons. $P < 0.05$ was considered to indicate a significant difference. Data were analyzed using the GraphPad Prism 5.0 software.

## 3 Results

### 3.1 Construction of protein-protein interaction network of HCM/hypertension and *A. bidentatae radix/S. chinensis*

Genes associated with "hypertrophic cardiomyopathy" and "hypertension" were analyzed using the GeneCards and

DisGeNET databases. By intersecting the search results, 62 disease-related target genes were identified (Fig. 1A, Table 1). Active components of *A. bidentatae radix* and *S. chinensis* were identified via the TCMSP online platform based on OB ≥ 30% and DL ≥ 0.18, resulting in the identification of 20 key active ingredients from *A. bidentatae radix* and 5 key active ingredients from *S. chinensis*, respectively (Table 2). The BATMAN database and SwissTargetPrediction database were then employed to predict targets of active ingredients, yielding a total of 696 target genes (Table S2). By intersecting the disease-related genes and active ingredient-related targets, 18 common targets were identified (Fig. 1B, Table S3).

GO functional analysis was performed on the 18 intersecting target genes. Top 10 enriched GO terms were obtained and visualized as bar chart (Fig. 1C), including "regulation of smooth muscle cell proliferation", "positive regulation of smooth muscle cell proliferation", "reactive nitrogen species metabolic process", "oxidoreductase activity", of which are closely linked with the pathological processes of HCM and hypertension. A network graph was then constructed to illustrate the relationships between the target genes and their associated GO functional terms (Fig. 1D).

### 3.2 Construction of herb-ingredient-target-pathway network

A pharmacological network was constructed to illustrate the pathway regulation mechanisms of key ingredients in the herbal formula, based on the herb-ingredient-target-pathway relationships. The network consisted of 2 herbs, 18 chemical component nodes, 18 target protein nodes, and 32 pathway nodes (Fig. 2, Table S4).

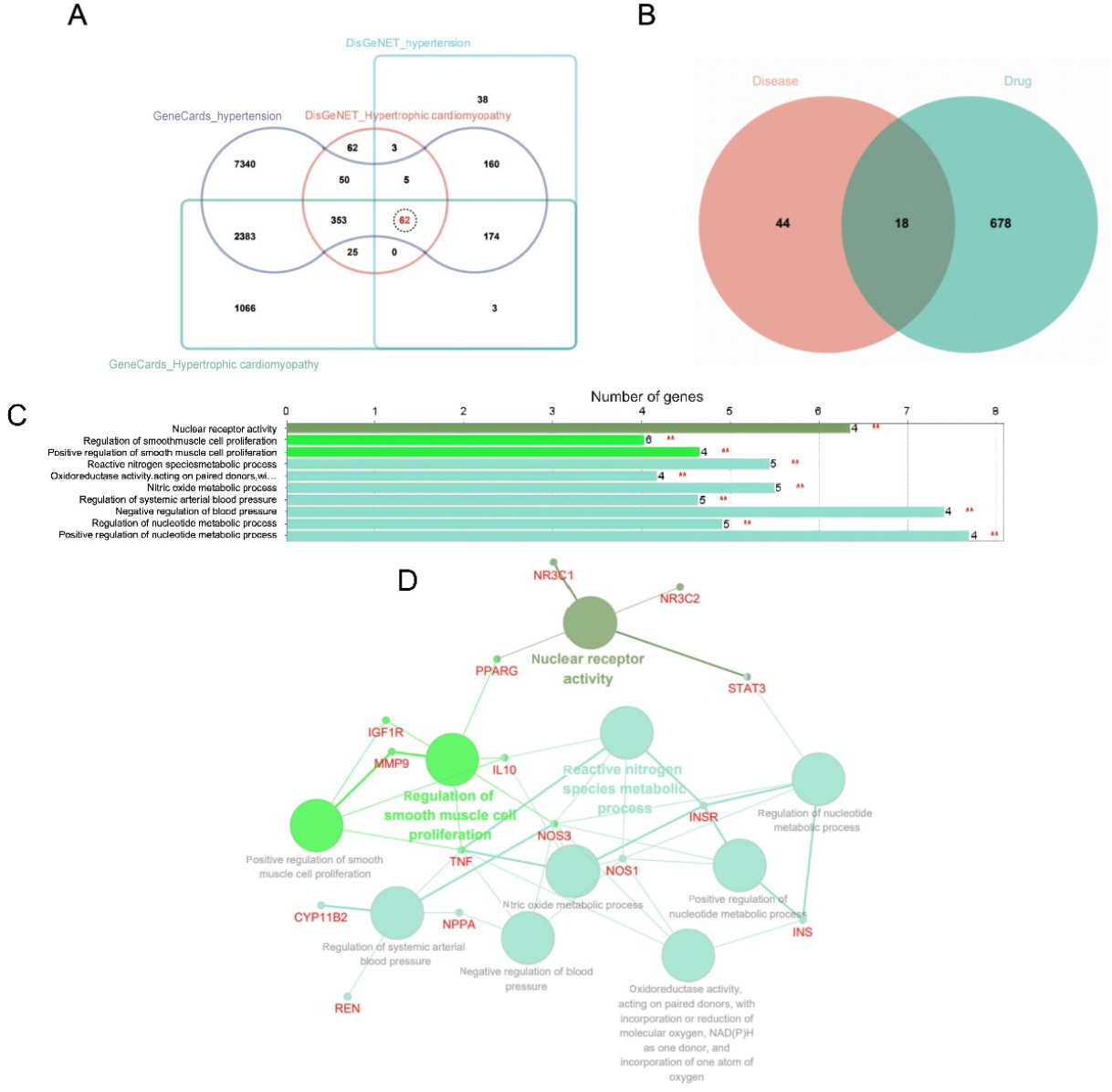



**Figure 1** Protein-protein interaction network of the food and medicine homological products of *A. bidentatae radix* and *S. chinensis* was established based on HCM and hypertension. (A) Venn diagram of genes associated with HCM and hypertension by separately utilized GeneCards and DisGeNET; (B) Venn diagram of intersecting target genes between "drug-disease" interactions; (C) Functional and signaling pathway enrichment network of target proteins. Based on ClueGO and CluePedia, a GO functional clustering analysis was performed for the target proteins. Bar chart of GO functional enrichment of target proteins; (D) The network graph in ClueGO is created based on the Kappa statistic, where each node represents a term, the connections between nodes reflect the relationships between terms, and the color of each node indicates its enrichment category (belonging to which functional group).

**Table 1** Common disease-related genes of "hypertrophic cardiomyopath" and "hypertension" in GeneCards and DisGeNet databases

| | | | | | |
|---|---|---|---|---|---|
| *SLC9A1* | *POMC* | *INS* | *EDN1* | *NPPA* | *CD36* |
| *NR3C2* | *GDF15* | *STAT3* | *SCN10A* | *VEGFA* | *TXN* |
| *REN* | *SYNE1* | *AGT* | *ACE* | *FTO* | *AGTR1* |
| *GJA1* | *NR3C1* | *IGF2* | *IGF1R* | *HMOX1* | *HLA-DPB1* |
| *MTPN* | *ADM* | *TGFB1* | *HLA-B* | *PPARG* | *LGALS3* |
| *TSC1* | *APLN* | *PLA2G7* | *ABO* | *GNAS* | *TNFRSF11B* |
| *CYP11B2* | *NPPB* | *IGF1* | *MIR29A* | *TNF* | *HLA-A* |
| *HFE* | *EDN2* | *PPARGC1A* | *AGTR2* | *ADRB1* | *CMA1* |
| *ACE2* | *NOS3* | *CRP* | *RETN* | *MMP9* | *IL10* |
| *MIR221* | *MIR21* | *LDLR* | *INSR* | *NPR1* | *NOS1* |
| *ATM* | *MYLK* | | | | |

Note: Totally 62 common disease-related genes among the intersection of "genecards-hypertrophic cardiomyopathy", "genecards-hypertension", "DisGeNet-hypertrophic cardiomyopathy", and "DisGeNet-hypertension".

### 3.3 Identification of key active ingredients of *A. bidentatae radix/S. chinensis* with key targets

The nodes within the network were identified and ranked according to their connectivity (Table S5). The 3D structures of these key nodes were retrieved as PDB files, and molecular docking studies were conducted by using AutoDock. This analysis resulted in four key docking interactions: quercetin with IGF1R (Fig. 3A), quercetin with INSR (Fig. 3B), inophyllum_E with INS (Fig. 3C), and quercetin with MMP9 (Fig. 3D).

### 3.4 Quercetin demonstrates a favorable binding with INSR

Molecular dynamics simulations were performed to assess the stability of interactions between proteins and active ingredient over 100 ns. The binding affinities of quercetin with IGF1R, INSR, and MMP9, as well as inophyllum_E with INS, were evaluated using metrics such as RMSD, hydrogen bonds, and binding free

**Table 2** Screening the active ingredients from *A. bidentata radix* and *S. chinensis* based on TCMSP

| TCMSP ID | Molecular name | OB | DL |
|---|---|---|---|
| | ***A. bidentata* radix** | | |
| MOL001006 | Poriferasta-7,22*E*-dien-3β-ol | 42.98 | 0.76 |
| MOL012461 | 28-Norolean-17-en-3-ol | 35.93 | 0.78 |
| MOL012505 | Bidentatoside,ii_qt | 31.76 | 0.59 |
| MOL012537 | Spinoside A | 41.75 | 0.4 |
| MOL012542 | β-Ecdysterone | 44.23 | 0.82 |
| MOL001454 | Berberine | 36.86 | 0.78 |
| MOL001458 | Coptisine | 30.67 | 0.86 |
| MOL000173 | Wogonin | 30.68 | 0.23 |
| MOL002643 | Δ7-Stigmastenol | 37.42 | 0.75 |
| MOL002714 | Baicalein | 33.52 | 0.21 |
| MOL002776 | Baicalin | 40.12 | 0.75 |
| MOL002897 | Epiberberine | 43.09 | 0.78 |
| MOL000358 | β-Sitosterol | 36.91 | 0.75 |
| MOL003847 | Inophyllum E | 38.81 | 0.85 |
| MOL000422 | Kaempferol | 41.88 | 0.24 |
| MOL004355 | Spinasterol | 42.98 | 0.76 |
| MOL000449 | Stigmasterol | 43.83 | 0.76 |
| MOL000785 | Palmatine | 64.6 | 0.65 |
| MOL000085 | β-Daucosterol | 36.91 | 0.75 |
| MOL000098 | Quercetin | 46.43 | 0.28 |
| | ***S. chinensis*** | | |
| MOL007980 | Saucernelignan-8 | 43.66 | 0.39 |
| MOL007981 | Saucernelignan-7 | 45.46 | 0.36 |
| MOL007984 | Δ5,22-Stigmastadien-3-ol | 43.83 | 0.76 |
| MOL007985 | Austrobailignan-5 | 42.54 | 0.38 |
| MOL000098 | Quercetin | 46.43 | 0.28 |
| MOL007980 | Saucernelignan-8 | 43.66 | 0.39 |

Note: Screen pricinples were set as OB ≥ 30% and DL ≥ 0.18 recorded in TCMSP.

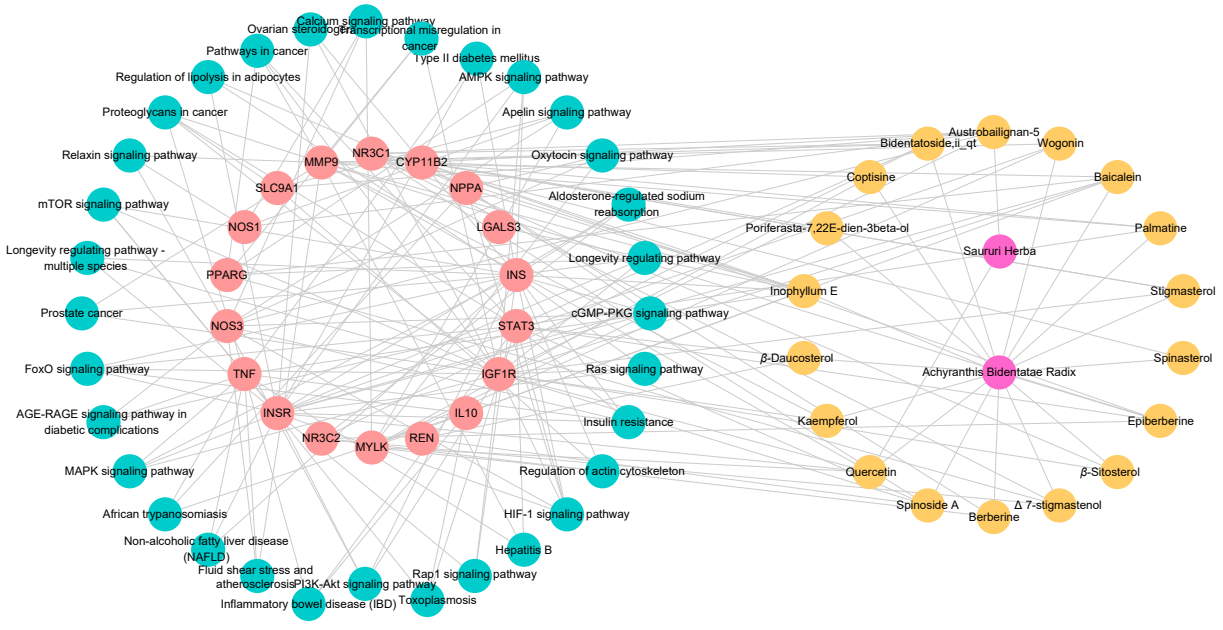



**Figure 2** Pharmacological network construction with *A. bidentatae radix/S. chinensis* and HCM/hypertension. Using the herb-active ingredient-target-pathway correspondence, a pharmacological network was constructed using Cytoscape. Totally 18 active ingredients nodes, 18 target protein nodes, and 32 pathway nodes were included, and the colors indicate herb (purple), compound (yellow), target protein gene (red), and KEGG pathway (blue).

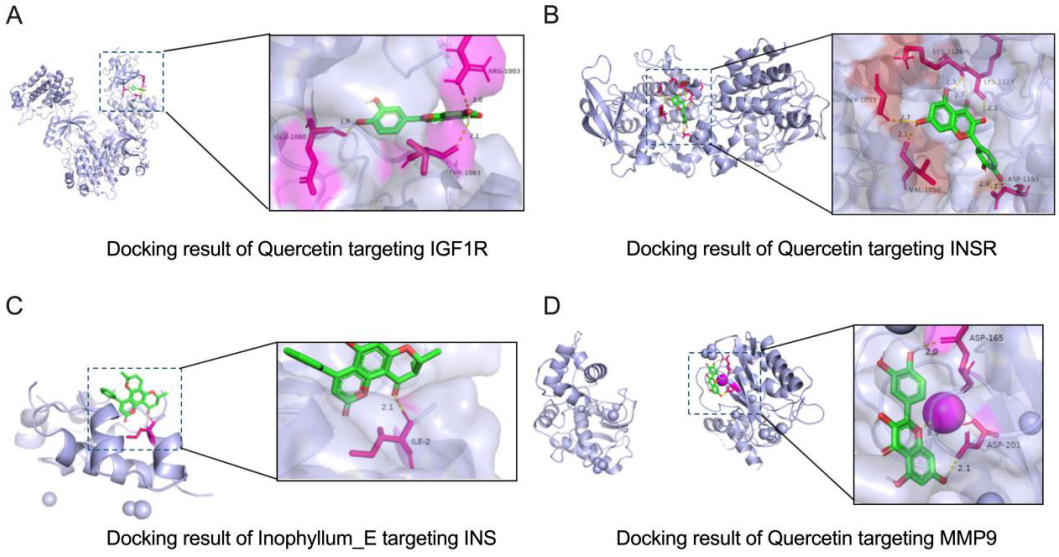



**Figure 3** Docking result of key composition from pharmacological network. (A-D) Docking images of quercetin/IGF1R, quercetin/INSR, inophyllum_E/INSR, and quercetin/MMP9, respectively.

energy. The RMSD analysis reveled that quercetin_INSR complex maintained a stable conformation throughout 30–100 ns simulation. The quercetin_IGF1R and quercetin_MMP9 complexes stabilized after 50 and 42 ns, respectively, with notable deviations from the RMSD of the protein monomers. In contrast, the inophyllum E_INS complex exhibited periodic fluctuations, indicating relative instability. Hydrogen bond analysis, conducted using Gromacs, showed that quercetin_IGF1R, quercetin_INSR, and quercetin_MMP9 formed 2–4 persistent hydrogen bonds (Fig. 4B). Notably, quercetin_INSR displayed significant and stable hydrogen bonding throughout the 100 ns simulation, with up to 6 hydrogen bonds at certain time points, suggesting a strong interaction between quercetin and INSR. Although inophyllum E_INS also formed continuous hydrogen bonds, the bond count was primarily limited to 2.

Binding free energy calculations using the MM-GBSA method provided further insights into the stability of the protein-ligand complexes. The results (Fig. 4C) indicated that quercetin_INSR and inophyllum E_INS had the lowest binding energies (<−20 kcal/mol), with quercetin_INSR showing the most favorable binding energy (<−33.71 kcal/mol). Residue-level decomposition of binding energy (Fig. 4D) revealed that Aspartic

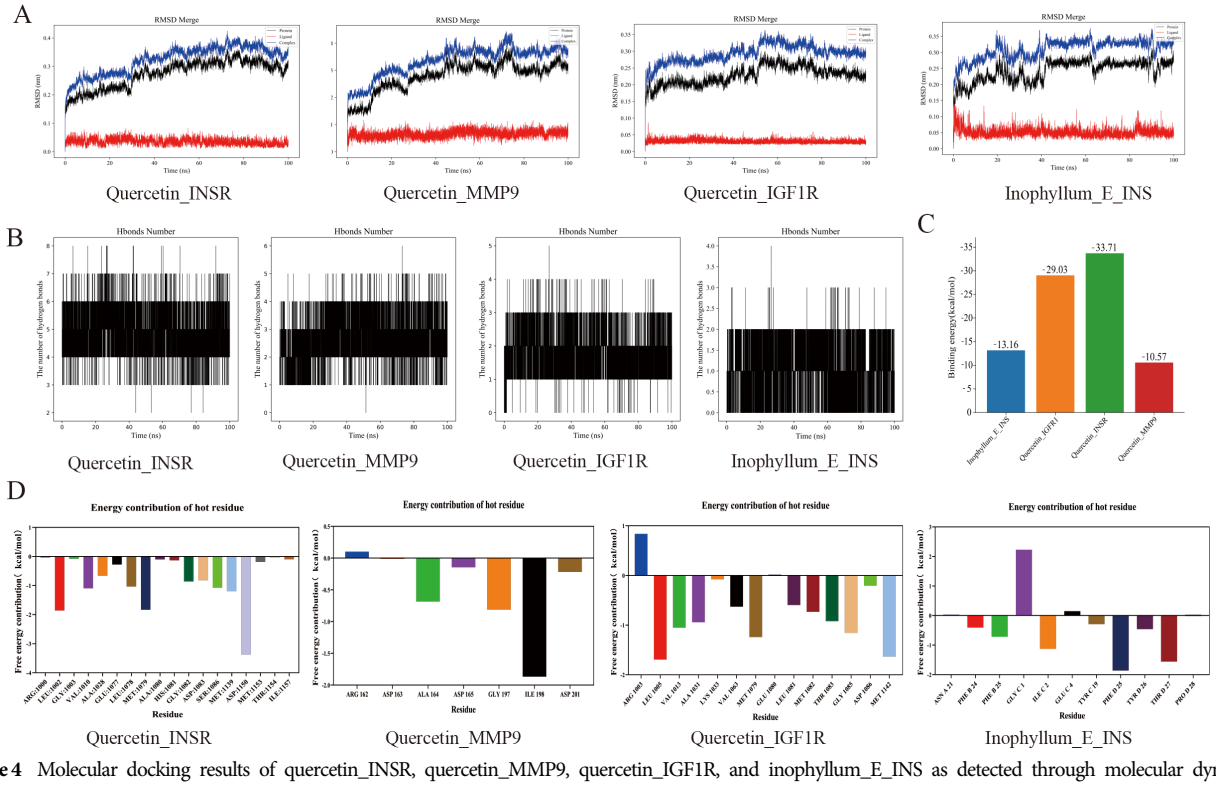



**Figure 4** Molecular docking results of quercetin_INSR, quercetin_MMP9, quercetin_IGF1R, and inophyllum_E_INS as detected through molecular dynamics simulations. (A) Analysis of RMSD values obtained from molecular dynamics simulations. Blue represents the complex of the small molecule with the protein, black represents the protein monomer, and red represents the RMSD values of the small molecule; (B) Analysis of hydrogen bond formation; (C) Analysis of binding energy; (D) Analysis of the contribution of amino acid residues to binding energy.

acid (ASP 1150) in the quercetin_INSR complex contributed significantly to binding stability (−3.373 kcal/mol), alongside other residues such as Leucine (LEU 1001) and Methionine (MET 1079). Conversely, in the other complexes, certain residues, such as Glycine (GLYC1) in inophyllum E_INS, Arginine (ARG 1003) in inophyllum E_IGF1R, and ARG 162 in inophyllum E_MMP9, contributed positively to the energy barriers, adversely affecting binding stability and leading to lower overall binding energies.

### 3.5 DL evaluation of quercetin and inophyllum_E

DL evaluations for quercetin and inophyllum_E were further conducted. The chemical structures of both ingredients are shown in Fig. 5. The results indicate that quercetin, a common active ingredient in *A. bidentatae radix* and *S. chinensis*, meets all DL criteria, exhibiting lower toxicity and favorable absorption, distribution, and excretion properties (Tables 3-5). Consequently, quercetin is identified as a promising lead ingredient in this study.

### 3.6 Pharmacological evaluations of quercetin in ameliorating HCM and hypertension

To validate the therapeutic potential of quercetin, target genes in Fig. 2 were examined using heart tissues from animal models of

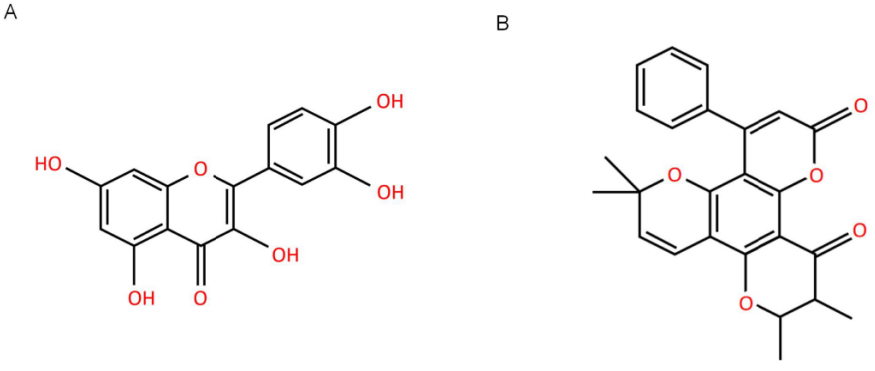



**Figure 5** Chemical structure of (A) quercetin and (B) inophyllum_E.

**Table 3** Comparison of physicochemical properties between quercetin and inophyllum_E

| Property | Quercetin | Inophyllum_E | Comments |
|---|---|---|---|
| Molecular weight | 302.04 | 402.15 | Contain hydrogen atoms.<br>Optimal: 100−500 |
| Number of hydrogen bond acceptors | 7 | 5 | Optimal: 0−12 |
| Number of hydrogen bond donors | 5 | 0 | Optimal: 0−7 |
| Number of rotatable bonds | 1 | 1 | Optimal: 0−11 |
| Number of rings | 3 | 5 | Optimal: 0−6 |
| Number of atoms in the biggest ring | 10 | 18 | Optimal: 0−18 |
| Number of heteroatoms | 7 | 5 | Optimal: 1−15 |
| Formal charge | 0 | 0 | Optimal: −4−4 |
| Number of rigid bonds | 18 | 29 | Optimal: 0−30 |
| Stereo centers | 0 | 2 | Optimal: ≤ 2 |
| TPSA | 131.36 | 65.74 | Topological polar surface area. Optimal: 0−140 |
| lg *S* | −3.671 | 5.738 | −lg of the aqueous solubility. Optimal: −4−0.5 lg (mol/L) |
| lg *P* | 2.155 | 5.517 | lg of the octanol/water partition coefficient.<br>Optimal: 0−3 |
| lg *D* | 1.767 | 4.41 | lg *P* at physiological pH 7.4<br>Optimal: 1−3 |

**Table 4** Comparison of drug-likeness of quercetin and inophyllum_E

| Property | Quercetin | Inophyllum_E | Comments |
|---|---|---|---|
| Lipinski Rule | Accepted | Accepted | $M_W \leq 500$; lg $P \leq 5$; Hacc ≤ 10; Hdon ≤ 5;<br>If two properties are out of range, a poor absorption or permeability is possible, one is acceptable |
| Pfizer rule | Accepted | Rejected | lg $P > 3$; TPSA < 75;<br>Compounds with a high lg $P$ (>3) and low TPSA (<75) are likely to be toxic |
| GSK rule | Accepted | Rejected | $M_W \leq 400$; lg $P \leq 4$;<br>Compounds satisfying the GSK rule may have a more favorable ADMET profile |
| Human intestinal absorption (HIA) | 0.014 | 0.011 | Value 1: HIA < 30%;<br>Value 0: HIA < 30%; |
| 20% bioavailability | 0.93 | 0.003 | Value 1: bioavailability < 20%;<br>Value 0: bioavailability ≥ 20%; |
| Fraction unbound in plasms (%) | 7.423 | 1.461 | Low: <5%;<br>Middle: 5%−20%;<br>High: >20% |
| Clearance | 8.284 | 2.353 | High: >15 mL/(min·kg); moderate: 5−15 mL/(min·kg);<br>low: <5 mL/(min·kg) |

**Table 5** Comparison of toxicity property evaluations of quercetin and inophyllum_E

| Property | Quercetin | Inophyllum_E | Comments |
|---|---|---|---|
| Human hepatotoxicity (HT) | 0.1 | 0.915 | Value 1: H-HT positive (+); Value 0: H-HT negative (–) |
| Drug induced liver injury (DILI) | 0.98 | 0.971 | Value 1: drugs with a high risk of DILI; Value 0: drugs with no risk of DILI |
| Rat oral acute toxicity | 0.065 | 0.947 | Value 1: high-toxicity; Value 0: low-toxicity |
| Carcinogen city | 0.05 | 0.858 | Value 1: carcinogens; Value 0: non-carcinogens |
| Respiratory toxicity | 0.072 | 0.659 | Value 1: high-toxicity; Value 0: low-toxicity |
| Environmental toxicity | 1.017 | 2.179 | Bioconcentration factors are used for considering secondary poisoning potential and assessing risks to human health via the food chain. The unit is –lg (mg/L) |
| Acute toxicity rule | 0 alert | 0 alert | Acute toxicity during oral administration |
| Genotoxic carcinogenicity rule | 0 alert | 1 alert | Carcinogenicity or mutagenicity |
| Aquatic toxicity rule | 0 alert | 0 alert | Toxicity to liquid (water) |
| SureChEMBL rule | 0 alert | 0 alert | MedChem unfriendly status |

hypertensive (L-NAME, ISO) and HCM (TAC). Given that bioinformatics predictions were made at the gene level, real time-PCR was employed to assess the expression levels of the genes predicted in the pharmacological network. Both HCM and hypertension resulted in the upregulation of the angiotensin system, such as NOS3, NPPA, NR3C1, consistent with pharmacological network prediction (Fig. 6A). We then evaluated the effects of various doses of quercetin[20], in the context of AngII

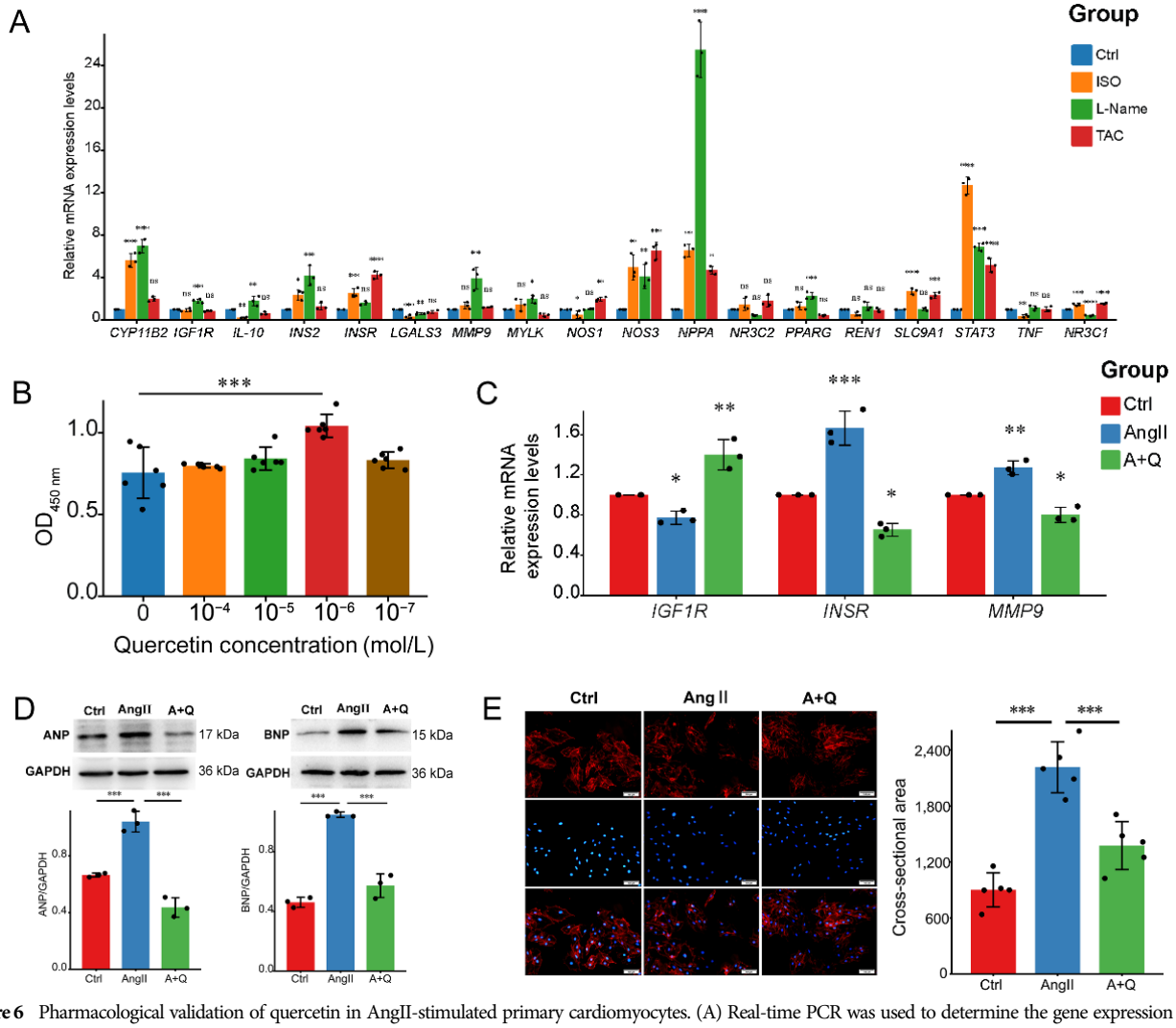



**Figure 6** Pharmacological validation of quercetin in AngII-stimulated primary cardiomyocytes. (A) Real-time PCR was used to determine the gene expression levels of *CYP11B2*, *IGF1R*, *IL-10*, *INS2*, *INSR*, *LGALS3*, *MMP9*, *MYLK*, *NOS1*, *NOS3*, *NPPA*, *NR3C2*, *PPARG*, *REN1*, *SLC9A1*, *STAT3*, *TNF* and *NR3C1* in animals heart tissue; (B) CCK8 analysis was used to detect the effect of PF on cell viability; (C) Real-time PCR was used to determine the expression levels of *IGF1R*, *INSR* and *MMP9* in cardiomyocyte; (D) Western blot was used to detect the expression levels of ANP and BNP protein in each batch ($n = 3$), ***$P < 0.001$; (E) WGA staining was used to detect the cell CSA for 24 h ($n = 5$), ***$P < 0.001$.

treatment, and identified a dose of $10^{-6}$ mol/L as effective (Fig. 6B), which was subsequently used for further experiments. The effects of quercetin on IGF1R, INSR, and MMP9 in primary isolated cardiomyocytes were examined, where it was observed that quercetin restored mRNA levels of these genes (Fig. 6C). Given that both HCM and hypertension are characterized by cardiac hypertrophy, we also assessed the impact of quercetin on cardiomyocyte cross-sectional area (CSA) and the protein levels of natriuretic peptide A (ANP) and natriuretic peptide B (BNP) (Figs. 6D, 6E), which are markers of myocardial hypertrophy. Quercetin effectively ameliorated AngII-induced cardiac hypertrophy, supporting the computational predictions and validating the reliability of our pharmacological network approach in identifying potential therapeutic components.

## 4 Discussion

Identifying effective treatments for specific diseases often requires filtering through numerous potential drug candidates. Bioinformatics and CADD techniques streamline this process by pinpointing promising therapeutic candidates from a vast array of compounds[21]. In our study, we employed these approaches to identify potential active ingredients in *A. bidentatae radix* and *S. chinensis* for the treatment of HCM and hypertension.

Our focus on hypertension and HCM stems from the understanding that blood pressure is a critical modifiable risk factor in the development and progression of HCM. Elevated blood pressure increases afterload, placing additional stress on the myocardium and leading to compensatory myocardial hypertrophy. Over time, this hypertrophy can exacerbate pathological changes associated with HCM, including left ventricular hypertrophy and fibrosis. By targeting blood pressure and its role in HCM pathogenesis, we aim to identify therapeutic strategies that can mitigate myocardial hypertrophy progression and improve clinical outcomes. This interconnectedness justifies our focus on these two diseases. Indeed, a one standard deviation increase in blood pressure is associated with a fourfold increase in HCM risk[22]. Hypertension not only imposes an increased workload on the heart but also leads to long-term myocardial damage, establishing a clear link with HCM[23]. HCM and hypertension share common etiological factors and pathological mechanisms. Familial aggregation and co-aggregation have been reported among patients with both conditions[24]. For example, truncating variants in the *ALPK3* gene are pathogenic causes of autosomal dominant HCM[25]. Sarcomere protein mutations are associated with earlier onset and a higher prevalence of familial HCM[26]. Moreover, high cholesterol and hyperlipidemia are common risk factors for both HCM and hypertension. Elevated myocardial infarction and hyperlipidemia levels in HCM patients are independent predictors of malignant arrhythmias and death[27]. In the general population, high LDL cholesterol is a known risk factor for hypertension[28]. Unhealthy lifestyle choices, such as poor diet, lack of physical activity, smoking, and excessive alcohol consumption, significantly increase the risk of both hypertension and HCM[26,27]. For instance, hypertensive smokers are more prone to severe forms of hypertension, including malignant and renovascular hypertension[29]. Additionally, passive smoking has been causally linked to hypertension and end-organ damage, with nicotine administration affecting cardiac contractility in HCM patients[30]. Exploring common etiological mechanisms can indeed pave the way for more effective prevention and intervention strategies for both diseases. However, current research in this area is limited, despite its potential for breakthroughs. This is a primary objective of our ongoing research, which seeks to deepen our understanding of potential treatment targets and strategies by investigating common mechanisms between hypertension and HCM. Our current study utilized bioinformatics and CADD for the high-throughput exploration of natural products and their active components with potential therapeutic effects.

Existing literature highlights the positive role of computer-based approaches in drug discovery and development, as exemplified by the COVID-19 therapeutic nirmatrelvir/ritonavir. For instance, PF-07321332, the core component of PAXLOVID, was designed based on the peptide rupintrivir and further optimized for OB[31]. These methods significantly contribute to discovering potential therapeutics not only for COVID-19 but also for various other conditions.

Our research centers on *S. chinensis* and *A. bidentatae radix* due to their known pharmacological effects in promoting blood circulation and eliminating blood stasis, as well as their demonstrated efficacy in treating rheumatic arthralgia according to TCM. Given the complex compositions of natural products, we employed molecular docking to identify key functional components. Quercetin and inophyllum_E showed positive docking results, directly interacting with IGF1R, INSR, MMP9, and INS. Research suggests that increased insulin/IGF signaling activation (e.g., INSR, IGF1R, AKT3, SGK1) contributes to myocardial hypertrophy and impaired cardiac function[32]. Angiotensin (1-7) exhibits anti-hypertensive and anti-proliferative properties, directly enhancing MMP-2 and MMP-9 activity[33]. Donohue syndrome, caused by mutations in the *INSR* gene, leads to non-functional insulin receptors and insulin resistance, characterized by hyperinsulinemia, HCM, and hypotonia[34]. Alterations in the INSR promoter are significantly linked to insulin levels and blood pressure, suggesting a causal relationship between compensatory hyperinsulinemia due to insulin resistance and hypertension[35]. Dysregulation of INSR signaling has been implicated in various cardiovascular diseases, including HCM and hypertension[36]. Indeed, the first molecular genetic association with hypertension involved the *INSR* gene[37]. Furthermore, the pro-hypertrophic response induced by mir15a/mir16-1 inhibition was abolished by knocking down INSR and IGF1R[38]. INSR dysfunction is intricately linked to the pathophysiology of both HCM and hypertension. Advances in molecular dynamics simulations provide valuable insights into the molecular underpinnings of these conditions and hold promise for developing targeted therapies that address the underlying causes of these cardiovascular diseases.

To validate our computational predictions, we conducted pharmacological verification experiments. Our study confirmed that quercetin significantly reduced cardiac hypertrophy, enhanced cell viability, and restored IGF1R, INSR, and MMP9 levels. This prompts further exploration of the molecular pathways through which quercetin exerts positive effects on cardiac health, and suggests the potential development of quercetin-based therapeutics for HCM and hypertension, offering new hope for patients suffering from these conditions.

However, our study has limitations. We focused on natural active ingredients from Achyranthes bidentata and *S. chinensis* to combat HCM and hypertension, leveraging their therapeutic effects as medicinal and edible homologous products. The idea is to integrate these herbs into daily diets once their active ingredients are identified. However, our research primarily relied on bioinformatics and CADD and lacks *in vivo* experimental

evidence with *A. bidentatae radix* and *S. chinensis*. Future studies should address this gap. Additionally, while we identified and validated promising genes like *IGF1R*, *INSR*, and *MMP9*, further in-depth mechanistic investigations of these genes are warranted.

In summary, our study provides a comprehensive investigation into the effects of *S. chinensis* and *A. bidentatae radix* on HCM and hypertension, contributing to methodological advancements in this field through effective predictive, screening, and evaluation frameworks.

## 5 Conclusion

This study employed computer-based methods, encompassing comprehensive bioinformatics data analysis and CADD, to investigate the therapeutic potential of *A. bidentatae radix* and *S. chinensis*. Furthermore, our research unveiled an active ingredient, quercetin, as the bioactive compound present in both herbs with potential targets of IGF1R, INSR, MMP9. This shared mechanism underscores the pharmacological efficacy of quercetin in alleviating symptoms associated with both HCM and hypertension.

## Conflicts of interest

The authors declare that there are no conflicts of interest in this work. Minhui Li and Hui Li are the associate editor of Food & Medicine Homology, but was not involved in the processing, peer review or decision making of this article.

## Acknowledgments

We appreciated Yanyan Zhang for the mice heart tissues of Control, ISO, L-NAME and TAC group. This work was supported by the grants from the National Natural Science Foundation of China (No. 82104173/82104169), Research Institute of Medicine & Pharmacy of Qiqihar (No. QMSI2022M-02), Research project of Health Commission of Heilongjiang Province (No. 20210202020361).

## Electronic Supplementary Material (ESM)

The online version contains supplementary material available at https://doi.org/10.26599/FMH.2026.9420103

## References

[1] Hamatani, Y., Amaki, M., Yonezawa, R., et al. Prevalence, determinants, and prognostic significance of exercise-induced pulmonary hypertension in patients with hypertrophic cardiomyopathy. *The International Journal of Cardiovascular Imaging*, **2019**, 35: 837–844. https://doi.org/10.1007/s10554-018-01522-4

[2] Kahan, T., Bergfeldt, L. Left ventricular hypertrophy in hypertension: its arrhythmogenic potential. *Heart*, **2005**, 91: 250–256. https://doi.org/10.1136/hrt.2004.042473

[3] Mohd Sairazi, N. S., Sirajudeen, K. N. S. Natural products and their bioactive compounds: neuroprotective potentials against neurodegenerative diseases. *Evidence-Based Complementary and Alternative Medicine*, **2020**, 2020: 6565396. https://doi.org/10.1155/2020/6565396

[4] Available from: https://m.pingguolv.com/zy/gongxiao/84249.html.

[5] Liu, J., Pan, J., Wang, Y., et al. Component analysis of Chinese medicine and advances in fuming-washing therapy for knee osteoarthritis via unsupervised data mining methods. *Journal of Traditional Chinese Medicine*, **2013**, 33: 686–691. https://doi.org/10.1016/s0254-6272(14)60043-1

[6] Wu, Y., Liu, J., Kang, S., et al. Rapid analysis of aristolochic acids and aristolactams in *Houttuyniae herba* by LC-MS/MS. *Molecules*, **2022**, 27: 5969. https://doi.org/10.3390/molecules27248969

[7] Han, H. J., Li, M., Son, J. K., et al. Sauchinone, a lignan from *Saururus chinensis*, attenuates neutrophil pro-inflammatory activity and acute lung injury. *International Immunopharmacology*, **2013**, 17: 471–477. https://doi.org/10.1016/j.intimp.2013.07.011

[8] Zhao, L., Zhang, H., Li, N., et al. Network pharmacology, a promising approach to reveal the pharmacology mechanism of Chinese medicine formula. *Journal of Ethnopharmacology*, **2023**, 309: 116306. https://doi.org/10.1016/j.jep.2023.116306

[9] Yang, W. Clinical efficacy of modified Sancao Jiangya decoction in the treatment of hypertension with hyperactive liver fire. *Inner Mongolia Traditional Chinese Medicine*, **2020**, 39: 6. https://doi.org/10.16040/j.cnki.cn15-1101.2020.02.006

[10] Xu, W., Zhu, F., Zhang, Y., et al. An overview of the treatments for hypertrophic cardiomyopathy. *Frontiers in Cardiovascular Medicine*, **2024**, 11: 1387596. https://doi.org/10.3389/fcvm.2024.1387596

[11] Ma Zheng. Treatment with modified Sancao antihypertensive decoction Clinical observation of hyperactive liver fire type hypertension. *China Naturopathy*, **2018**, 26: 28–30. https://doi.org/10.19621/j.cnki.11-3555/r.2018.0817

[12] Chen, Y. R., Niu, Y. S., Zhou, H. L. Achyranthes bidentata Blume (Amaranthaceae): a review of its botany, traditional uses, phytochemistry, pharmacology, and toxicology. *Journal of Pharmacy and Pharmacology*, **2024**, 76: 930–966. https://doi.org/10.1093/jpp/rgae012

[13] Li, S., Zhang, B. Traditional Chinese medicine network pharmacology: theory, methodology and application. *Chinese Journal of Natural Medicines*, **2013**, 11: 110–120. https://doi.org/10.1016/s1875-5364(13)60037-0

[14] Pinzi, L., Rastelli, G. Molecular docking: shifting paradigms in drug discovery. *International Journal of Molecular Sciences*, **2019**, 20: 4331. https://doi.org/10.3390/ijms20184331

[15] Yang, S. Y. Pharmacophore modeling and applications in drug discovery: challenges and recent advances. *Drug Discovery Today*, **2010**, 15: 444–450. https://doi.org/10.1016/j.drudis.2010.03.013

[16] Zhang, Y., Luo, M., Wu, P., et al. Application of computational biology and artificial intelligence in drug design. *International Journal of Molecular Sciences*, **2022**, 23: 3568. https://doi.org/10.3390/ijms232113568

[17] Ambure, P., Roy, K. CADD modeling of multi-target drugs against Alzheimer's disease. *Current Drug Targets*, **2017**, 18: 522–533. https://doi.org/10.2174/1389450116666150907104855

[18] Meanwell NA. Improving drug candidates by design: a focus on physicochemical properties as a means of improving compound disposition and safety. *Chem Res Toxicol*. **2011** Sep 19;24(9):1420–56. Epub 2011 Jul 26. PMID: 21790149. https://doi.org/10.1021/tx200211v

[19] Xiao, D., Zhang, Y., Wang, R., et al. Emodin alleviates cardiac fibrosis by suppressing activation of cardiac fibroblasts via upregulating metastasis associated protein 3. *Acta Pharmaceutica Sinica B*, **2019**, 9: 724–733. https://doi.org/10.1016/j.apsb.2019.04.003

[20] Lin, X., Zhao, X., Chen, Q., et al. Quercetin ameliorates ferroptosis of rat cardiomyocytes via activation of the SIRT1/p53/SLC7A11 signaling pathway to alleviate sepsis-induced cardiomyopathy. *International Journal of Molecular Medicine*, **2023**, 52: 5319. https://doi.org/10.3892/ijmm.2023.5319

[21] Dong, Y., Zhao, Q., Wang, Y. Network pharmacology-based investigation of potential targets of astragalus membranaceous-angelica sinensis compound acting on diabetic nephropathy. *Scientific Reports*, **2021**, 11: 19496. https://doi.org/10.1038/s41598-021-98925-6

[22] Harper, A. R., Goel, A., Grace, C., et al. Common genetic variants and modifiable risk factors underpin hypertrophic cardiomyopathy

susceptibility and expressivity. *Nature Genetics*, **2021**, 53: 135–142. https://doi.org/10.1038/s41588-020-00764-0

[23] Zheng, X., He, Z., Li, M., et al. Global research trends of hypertrophic cardiomyopathy from 2000 to 2022: insights from bibliometric analysis. *Frontiers in Cardiovascular Medicine*, **2023**, 10: 1039098. https://doi.org/10.3389/fcvm.2023.1039098

[24] Kondo, T., Toyoshima, H., Tsuzuki, Y., et al. Familial aggregation and coaggregation of history of hypertension and stroke. *Journal of Human Hypertension*, **2005**, 19: 119–125. https://doi.org/10.1038/sj.jhh.1001788

[25] Lopes, L. R., Garcia-Hernández, S., Lorenzini, M., et al. Alpha-protein kinase 3 (ALPK3) truncating variants are a cause of autosomal dominant hypertrophic cardiomyopathy. *European Heart Journal*, **2021**, 42: 3063–3073. https://doi.org/10.1093/eurheartj/ehab424

[26] Elliott, P. M., Anastasakis, A., Borger, M. A., et al. 2014 ESC Guidelines on diagnosis and management of hypertrophic cardiomyopathy: the Task Force for the Diagnosis and Management of Hypertrophic Cardiomyopathy of the European Society of Cardiology (ESC). *European Heart Journal*, **2014**, 35: 2733–2779. https://doi.org/10.1093/eurheartj/ehu284

[27] Mancia, G., Fagard, R., Narkiewicz, K., et al. 2013 ESH/ESC guidelines for the management of arterial hypertension: the Task Force for the Management of Arterial Hypertension of the European Society of Hypertension (ESH) and of the European Society of Cardiology (ESC). *European Heart Journal*, **2013**, 34: 2159–2219. https://doi.org/10.1093/eurheartj/eht151

[28] Cicero, A. F. G., Fogacci, F., Giovannini, M., et al. Interaction between low-density lipoprotein-cholesterolaemia, serum uric level and incident hypertension: data from the Brisighella Heart Study. *Journal of Hypertension*, **2019**, 37: 728–731. https://doi.org/10.1097/hjh.0000000000001927

[29] Virdis, A., Giannarelli, C., Neves, M. F., et al. Cigarette smoking and hypertension. *Current Pharmaceutical Design*, **2010**, 16: 2518–2525. https://doi.org/10.2174/138161210792062920

[30] Gaffin, R. D., Chowdhury, S. A., Alves, M. S., et al. Effects of nicotine administration in a mouse model of familial hypertrophic cardiomyopathy, $\alpha$-tropomyosin D175N. *American Journal of Physiology-Heart and Circulatory Physiology*, **2011**, 301: H1646–1655. https://doi.org/10.1152/ajpheart.00277.2010

[31] Owen, D. R., Allerton, C. M. N., Anderson, A. S., et al. An oral SARS-CoV-2 M(pro) inhibitor clinical candidate for the treatment of COVID-19. *Science*, **2021**, 374: 1586–1593. https://doi.org/10.1126/science.abl4784

[32] Guo, H., Ma, K., Hao, W., et al. mir15a/mir16-1 cluster and its novel targeting molecules negatively regulate cardiac hypertrophy. *Clinical and Translational Medicine*, **2020**, 10: e242. https://doi.org/10.1002/ctm2.242

[33] Pei, Z., Meng, R., Li, G., et al. Angiotensin-(1-7) ameliorates myocardial remodeling and interstitial fibrosis in spontaneous hypertension: role of MMPs/TIMPs. *Toxicology Letters*, **2010**, 199: 173–181. https://doi.org/10.1016/j.toxlet.2010.08.021

[34] Perge, K., Massoud, M., Gauthier-Moulinier, H., et al. Intrauterine growth restriction and hypertrophic cardiomyopathy as prenatal ultrasound findings in a case of Leprechaunism. *Molecular Syndromology*, **2020**, 11: 223–227. https://doi.org/10.1159/000509837

[35] Dahale, S., Ruiz-Orera, J., Silhavy, J., et al. Cap analysis of gene expression reveals alternative promoter usage in a rat model of hypertension. *Life Science Alliance*, **2022**, 5. https://doi.org/10.26508/lsa.202101234

[36] Wang, Y., Li, J., Xiang, Q., et al. INSR and ISR-1 gene polymorphisms and the susceptibility of essential hypertension: a meta-analysis. *Experimental and Therapeutic Medicine*, **2023**, 25: 251. https://doi.org/10.3892/etm.2023.11950

[37] Morris, B. J. Insulin receptor gene in hypertension. *Clinical and Experimental Hypertension*, **1997**, 19: 551–565. https://doi.org/10.3109/10641969709083169

[38] Besnier M, Shantikumar S, Anwar M, Dixit P, Chamorro-Jorganes A, Sweaad W, Sala-Newby G, Madeddu P, Thomas AC, Howard L, Mushtaq S, Petretto E, Caporali A, Emanueli C. miR-15a/-16 Inhibit Angiogenesis by Targeting the Tie2 Coding Sequence: Therapeutic Potential of a miR-15a/16 Decoy System in Limb Ischemia. *Mol Ther Nucleic Acids*. **2019** Sep 6; 17: 49–62. Epub 2019 May 17. PMID: 31220779. https://doi.org/10.1016/j.omtn.2019.05.002